NANO LETTERS

2008
Vol. 8, No. 2
601−605

Excitation of Local Field Enhancement on Silicon Nanowires

Linyou Cao,[†] Bora Garipcan,[†,‡] Eric M. Gallo,[§] Stephen S. Nonnenmann,[†] Bahram Nabet,[†,§] and Jonathan E. Spanier*[,†,§]

Department of Materials Science and Engineering, Department of Electrical and Computer Engineering, Drexel University, Philadelphia Pennsylvania 19104, and Department of Chemical Engineering, Bioengineering Division, Hacettepe University, Beytepe, Ankara, 06800, Turkey

Received November 16, 2007; Revised Manuscript Received December 27, 2007

ABSTRACT

The interaction between light and reduced-dimensionality silicon attracts significant interest due to the possibilities of designing nanoscaled optical devices, highly cost-efficient solar cells, and ultracompact optoelectronic systems that are integrated with standard microelectronic technology. We demonstrate that Si nanowires (SiNWs) possessing metal-nanocluster coatings support a multiplicatively enhanced near-field light-matter interaction. Raman scattering from chemisorbed probing molecules provides a quantitative measure of the strength of this enhanced coupling. An enhancement factor of 2 orders of magnitude larger than that for the surface plasmon resonance alone (without the SiNWs) along with the attractive properties of SiNWs, including synthetic controllability of shape, indicates that these nanostructures may be an attractive and versatile material platform for the design of nanoscaled optical and optoelectronic circuits.

The large enhancement of the optical near-field close to illuminated particles when the incident wavelength is resonant with natural electromagnetic eigenmodes of the particle has long been recognized and proposed for numerous applications.[1] It has most recently been exploited in optical antennas for high-bandwidth intrachip and interchip connections and has potential to dramatically improve the efficiency in harvesting energy from solar radiation.[2−5] Most research efforts have focused on excitation of the surface plasmon resonance (SPR) on metallic nanostructures, particularly Au, Ag, and Cu.[6−12] However, the local response of nonmetallic nanostructures to electromagnetic radiation and its possible applications are also of considerable interest, due in part to the fact that dielectrics have weaker damping, resulting in a higher efficiency in radiative transfer.[13,14]

We demonstrate this for Si nanowires (SiNWs) by calculating the spatial dependence of the optical field outside the surface of a cylindrical nanowire of radius R illuminated by a monochromatic plane wave of wavelength λ with arbitrary electric field polarization (see Figure S1 within §S1 of the Supporting Information). Solution of Maxwell's equations and application of appropriate boundary conditions at the dielectric nanowire-vacuum interface (eq s1 in §S1 of the Supporting Information) allows the local optical field E_{ext}^{NW} to be expressed using the Lorenz−Mie formalism in cylindrical coordinates (r, θ, z). Resonance occurs when λ approaches one of the natural electromagnetic modes of the nanowire.[15] Considering a SiNW under monochromatic plane-wave excitation (without loss of generality) with the incident electric field-polarized parallel (TM) or perpendicular (TE) to the axis of the nanowire, the spatial distributions of the calculated near-field intensity $I_{ext}^{NW} = |E_{ext}^{NW}|^2$ (see eq s4 in §S1 of the Supporting Information) for the cases of resonant and nonresonant conditions (Figure 1) clearly demonstrate that the local field at resonance (Figure 1a) is strongly confined to near the surface of the SiNW with the intensity enhanced by ∼20-fold, while the nonresonant field (Figure 1b) is weaker by 1 order of magnitude and is delocalized over a range of hundreds of nanometers away from the surface. Compared to the surface plasmon resonance-enhanced field that is significantly attenuated beyond a molecular-scale distance away from the metallic substrate,[16] the resonant local field at the dielectric surface is expected to be much longer ranging in enhancing optical emission,[17,18] absorption,[19] optical force,[20] and nonlinear optical response of mesoscopic systems[21,22] as it extends over tens of nanometers (Figure 1a).

Here, we focus on the average intensity of the local field $\overline{I_{ext}^{NW}}$ obtained by integration over the surface of the nanowire ($\overline{I_{ext}^{NW}} = (2\pi)^{-1}\int_0^{2\pi} |E_{ext}^{NW}|^2 \, d\theta$, see eq s5 in §S1 of the Supporting Information). The local light-matter interaction at the surface of the nanowire can be evaluated experimen-

* To whom correspondence should be addressed. E-mail: spanier@drexel.edu.
† Department of Materials Science and Engineering, Drexel University.
‡ Hacettepe University.
§ Department of Electrical and Computer Engineering, Drexel University.

10.1021/nl0729983 CCC: $40.75
Published on Web 01/26/2008

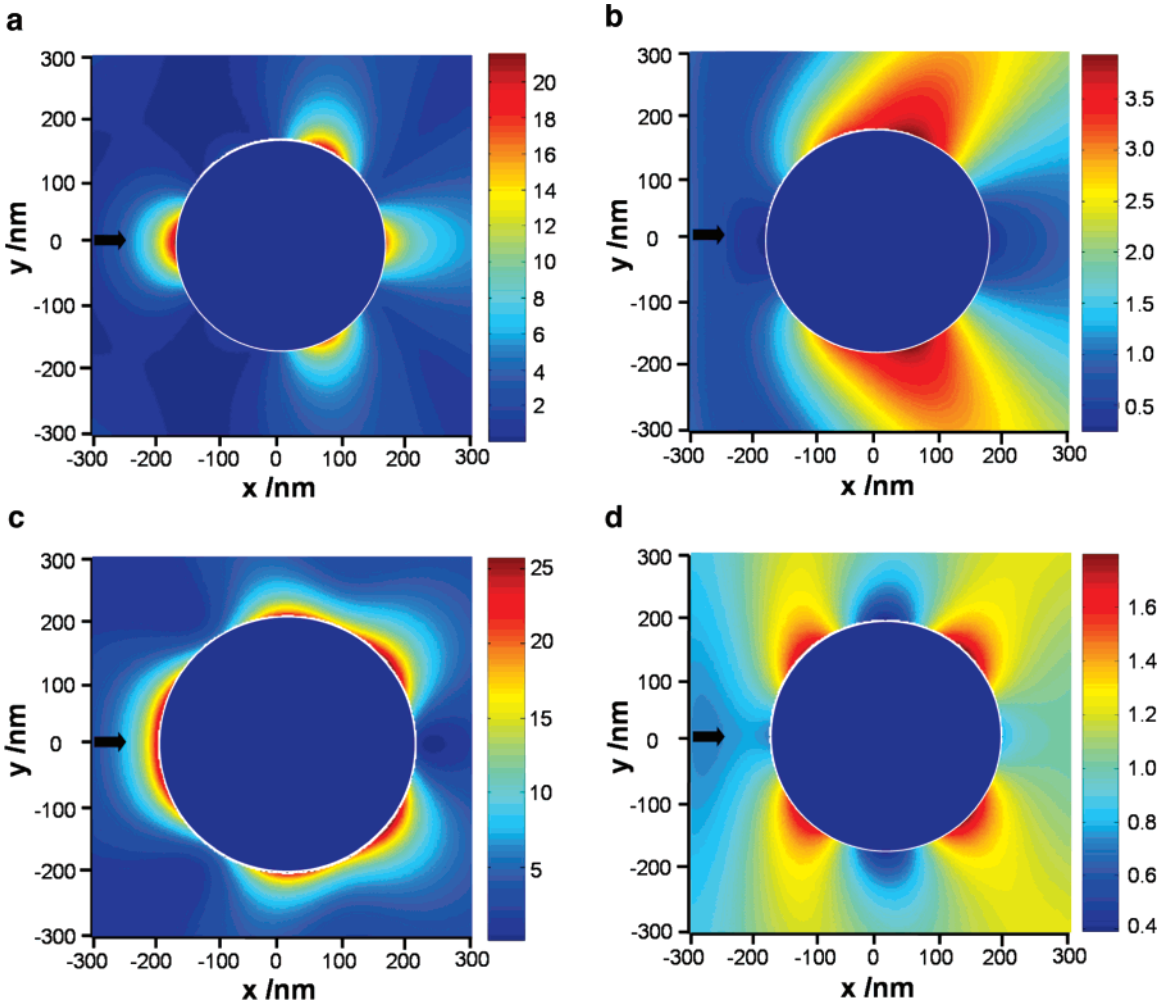

Figure 1. Spatial distribution of the optical near-field in the vicinity of a SiNW (calculated, cross-sectional view). Normally incident, monochromatic ($\lambda = 785$ nm) plane-wave radiation of unity intensity is denoted by the black arrow. (a) Resonant scattering and (b) nonresonant scattering for TM-mode excitation of SiNWs possessing radii of 169.3 and 179.8 nm, respectively. (c) Resonant scattering and (d) nonresonant scattering for TE mode excitation corresponding to radii of 180.2 and 208.7 nm, respectively The surface of each SiNW is denoted by a white circle, and the intensity of the internal field is intentionally set to zero for clarity. The nonresonant near-field extends to more than 300 nm from the surface, exceeding the area of the figure. The employed complex refractive index of silicon is $3.691-0.005\,i$.[23] The calculated resonant responses in panels a and c are shown for $n = 3$, where n is subscript in the scattering coefficients a_n and b_n as defined in eq s2 in §S1 of the Supporting Information.

tally by monitoring selected optical signals such as the Raman scattering from chemisorbed molecules. Using the wavelength-dependent complex dielectric permittivity for Si,[23] calculated values of $\overline{I_{ext}^{NW}}$ as functions of the SiNW radius R and of λ (Figure 2) reveal a series of sharp peaks that arise from resonant scattering.

The experimental proof of the predicted local field enhancement for SiNWs is carried out by collection of the Raman scattering from *p*-aminothiophenol (PATP) molecules chemisorbed onto Au nanoclusters (AuNCs) that form following vacuum thermal evaporation of Au onto the SiNWs (Figure 3a). Tapered SiNWs were prepared by metal nanostructure-catalyzed chemical vapor deposition as described elsewhere.[24] Au nanoclusters were formed reproducibly on as-prepared tapered SiNWs (and on 300 nm SiO_2-coated Si(100) wafers without SiNWs as blank control substrates) via thermal evaporation of Au. The adsorption of organic molecules was carried out by immersing AuNC-coated tapered SiNWs (as well as control substrates) in 1 wt % ethanol solution of PATP (Aldrich) for 24 h. Raman-scattering spectra of the self-assembled PATP monolayers were collected in the backscattering configuration with 632.8 nm HeNe (0.8 mW) and alternatively, 785 nm diode (0.08 mW) laser excitation focused to Gaussian spot diameters of $\sim$1.2 and $\sim$1.5 μm, respectively. The incident electric field was polarized perpendicular (TE), and alternatively, parallel (TM) to the long axis of the tapered SiNWs. Spectra were collected from a number of locations from the base to near the tip of each tapered SiNW, where the diffraction-limited spot size limited precision of the placement of the incident beam to $\sim \lambda/2$. For each λ and each nanostructure, the ratio of Stokes-to-anti-Stokes-scattered intensity was evaluated to ensure that no laser-induced heating occurred. All integrated intensities are the result of Lorentzian fittings of the measured lineshapes. All values of enhancement reported here were obtained from spectra collected from different locations along an individual tapered SiNW; the results from the tapered SiNW presented here are representative of all tapered SiNWs

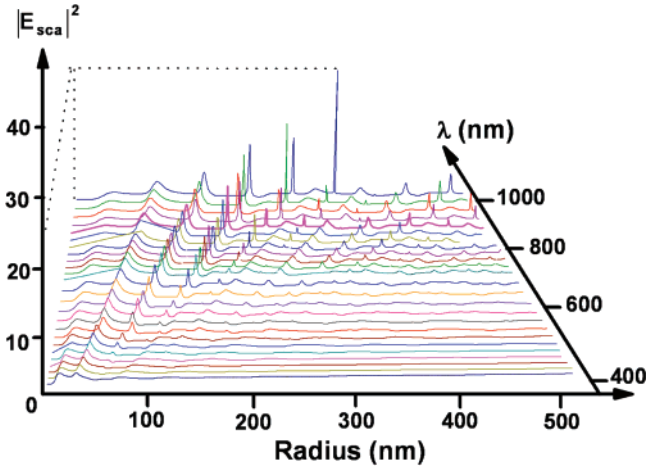

Figure 2. Evolution of the average intensity of the local surface field of a SiNW as a function of the radius and the incident wavelength λ (calculated). The calculation covers a wavelength range from 400 to 1000 nm. The maximum integrated intensity of the near-field is seen to increase from ~3.5 at $\lambda = 400$ nm to ~26 at $\lambda = 1000$ nm for corresponding radii of ~25 and ~320 nm, respectively. Variations in the intensity of the peaks depend in part on the wavelength-dependent complex dielectric function of Si, as the stronger absorption of silicon for shorter wavelength tends to dampen the resonant character.[23]

studied. Raman-scattering signals from bulk PATP with a thickness of 300 μm were also collected using identical conditions.

In the experiments, one can describe the role of the AuNCs as signal carriers: their SPRs along with the light-scattering resonant field together provide an enhancement that enables probing of the local light-matter interaction at the SiNW. The total field enhancement for this AuNCs−SiNW structure Q_{tot}^{NW} can be approximated as the product of the field enhancement from AuNCs Q_{Au} and that from the SiNW Q_{Si}^{NW}, that is, $Q_{tot}^{NW} = Q_{Au}(Q_{Si}^{NW})^2$ with the SiNW enhancing both the excitation of and the scattered radiation from the AuNCs (see §S2 of the Supporting Information). Because an enhanced field will also result in an increased polarization for the Raman-shifted frequency, the enhancement for the Raman-scattering intensity of PATP is proportional to the square of the field enhancement, $RE^{NW} = (Q_{tot}^{NW})^2 = (Q_{Au})^2(Q_{Si}^{NW})^4$.[15] Therefore, by factoring out the contribution to the Raman enhancement arising from the SPR of the AuNCs$(Q_{Au})^2$, one can assess the contribution$(Q_{Si}^{NW})^4$, that is, the field enhancement Q_{Si}^{NW} arising from the SiNW. Thus, the intensities of the measured Raman scattering from PATP chemisorbed onto AuNCs evaporated onto the tapered SiNW are normalized to that from PATP on identically prepared AuNCs evaporated onto a bulk crystal Si wafer under identical conditions, as shown in the scatter points in Figure 4. The samples probed are as-grown tapered SiNWs possessing an average apex angle of ~6° and length of ~25 μm (Figure 3d) coated by thermally evaporated AuNCs of average size 15.5 ± 5.0 nm with a nanocluster number density on the order of $\sim 10^{11}$ cm^{-2} (Figure 3b−d) onto which a monolayer of PATP is deposited, resulting in an estimated molecular number density of $\sim 2.56 \times 10^{18}$ cm^{-2}.[25]

The measured Raman scattered intensities for PATP chemisorbed on the AuNCs deposited on the SiNW are much larger than those for the molecules on the planar substrate (Figure 3d). To quantify the enhancement in the Raman scattering associated with the local field at the surface of the AuNCs-coated SiNW, we compared the measured Raman signal from the PATP molecules chemisorbed on the AuNCs on the SiNWs to that for bulk PATP. Normalizing to the bulk response, the effective values of Raman enhancement for the 1079 cm^{-1} peak are estimated to be $\sim 1.4 \times 10^6$, $\sim 5.8 \times 10^6$, $\sim 3.0 \times 10^7$, and $\sim 1.0 \times 10^8$ for the spectrum collected from the planar substrate and for different locations along the tapered SiNW, respectively, as denoted by arrows in Figure 3d. As discussed previously, this diameter-dependent variation in the Raman enhancement arises from the SiNW, and it allows us to establish the contribution $(Q_{Si}^{NW})^4$ or the local field enhancement Q_{Si}^{NW} resulting from the SiNW. In terms of light scattering, a gently tapered SiNW can be considered a chain of uniform diameter SiNWs with continuous change in size,[26] thereby facilitating the studies on the size-dependence of the optical near-field. Raman spectra collected at selected probing locations from the base to near the tip of a single tapered SiNW are plotted as a function of R in Figure 3e. We note that the variations in response for two different excitation wavelengths ($\lambda = 785$ and 632.8 nm, Figure 3e) are consistent with previous results for the intensity of the Raman scattering by optical phonons (520 cm^{-1}) in the SiNW alone.[26]

To compare our experimental results with theory, we recall the prediction (Figure 2) calculated from $\overline{I_{ext}^{NW}}$ $(= Q_{Si}^{NW})$ and plot the contributions to the calculated RE due to the SiNW as functions of R, along with the corresponding experimental results, for the two excitation wavelengths, 632.8 and 785 nm, TM-polarized excitation (Figure 4). Similar results were obtained for TE-polarized excitation (see Supporting Information, Figure S2). Because the experimental results shown involve a normalization of the RE for PATP from Au-modified SiNWs to that for the molecules from Au-modified planar silicon RE^{NW}/RE^{Pl}, our analysis also accounts for the imaging effect of the planar substrate $(Q_{Si}^{NW}/Q_{Si}^{Pl})^4$ (see §S2 of the Supporting Information). As seen in Figure 4, the diameter- and wavelength-dependences in our model calculations agree well with the experimental data.

There is some disagreement, however, between the model calculations and the experimental results. For example, the latter do not exhibit the undulations with R that are seen in the former. This may be due to one or more factors, including crystalline defects,[27] surface roughness,[28] and differences between our model description of the incident radiation and that for a realistic laser,[29] and that of the multiple scattering between the AuNCs and the SiNW. Although a refinement of the model or a different model approach could be developed to better address the electromagnetic interaction between the tapered SiNW and AuNCs,[30] the essential overall agreement verifies the light-scattering resonance-enhanced nature of the local field at the surface of the tapered SiNW.

The extra enhancement in the Raman scattering by chemisorbed molecules along with the model calculations presented here suggest a new paradigm for the use of

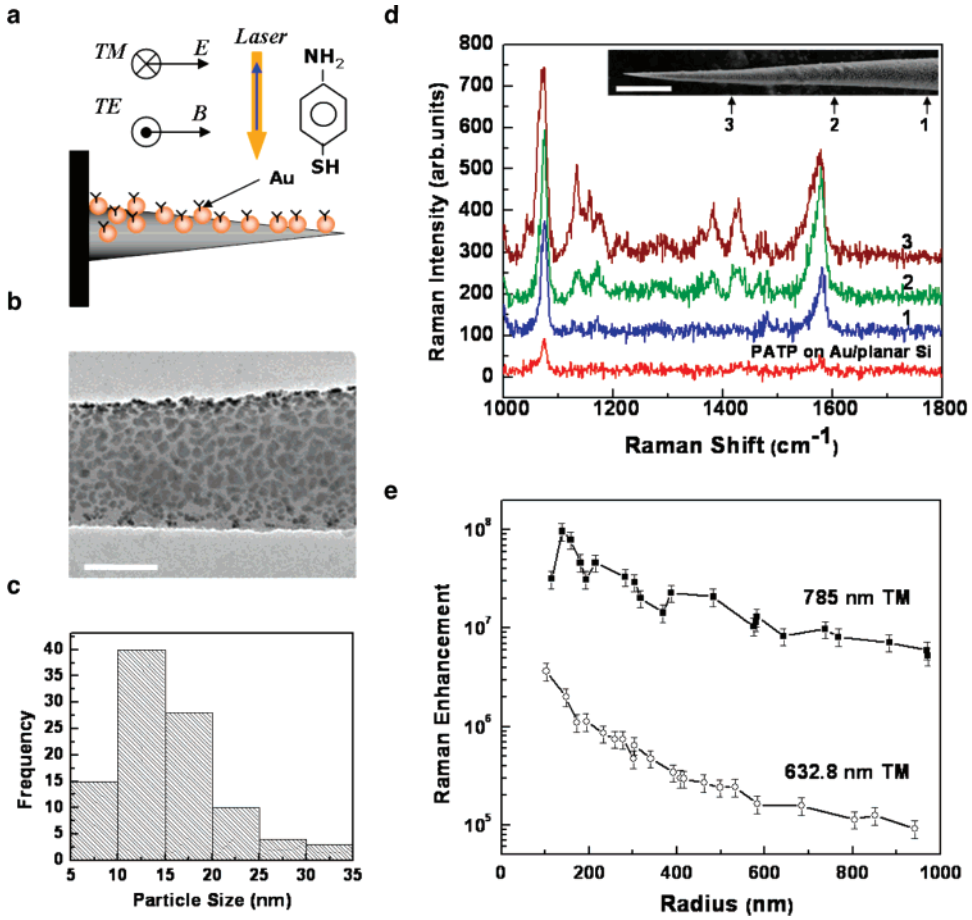

Figure 3. Raman-scattering measurements. (a) Schematic of experimental setup. The Raman spectra of PATP molecules that self-assemble onto Au nanocluster-coated and tapered SiNWs are collected in the backscattering geometry with TE and alternatively TM-polarized incident radiation. (b) A representative transmission electron micrograph (collected using a JEOL-2010F) of Au nanocluster-coated tapered SiNW; the scale bar is 100 nm. This, along with other TEM (not shown), confirms that the density of the Au nanoclusters is on the order of $\sim 10^{11}$ cm^{-2} for each of the regions of the tapered SiNWs probed. (c) Histogram of the size of the Au nanoclusters. (d) Raman spectra of PATP collected from the planar substrate and various locations along the tapered SiNW as denoted in the figure using 785 nm laser excitation. The inset is a scanning electron micrograph (obtained using Amray 1850FE) of a portion of the Au nanocluster-coated tapered SiNW; the scale bar is 2 μm. (e) Evolution of the Raman enhancement for the PATP molecules chemisorbed onto Au nanocluster (Au NC)-modified SiNWs as a function of the radius of the SiNWs collected using 632.8 (open circle) and 785 nm (solid square) with TM-polarized incident laser excitation as detailed in the main text. The estimated enhancements in the Raman scattered intensities for the molecules chemisorbed on the Au nanocluster-modified planar Si substrate are $\sim 1.6 \times 10^5$ and $\sim 1.4 \times 10^6$ for 632.8 and 785 nm light, respectively.

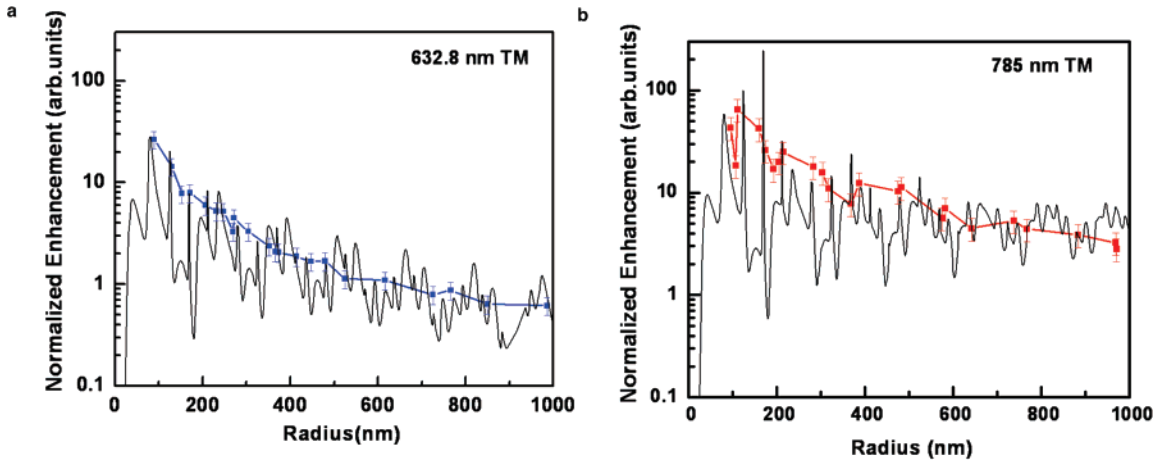

Figure 4. Comparison of calculated and experimentally observed enhancement. Results shown are for TM-polarized excitation of wavelengths (a) 632.8 and (b) 785 nm (for results for TE excitation see Supporting Information, Figure S2). The experimental results shown (color, scatter) were obtained by normalizing the Raman enhancement of PATP chemisorbed onto the Au NCs/SiNW to that for the molecules on Au/planar Si, RE^{NW}/RE^{Pl}. The calculated results shown (color, solid black line) were obtained by normalizing the calculated light-scattering resonance-induced enhancement arising from tapered SiNWs to the enhancement resulting from the imaging effect of the planar silicon, $(Q_{Si}^{NW}/Q_{Si}^{Pl})^4$ (see Supporting Information, §S2).

uniform-diameter and tapered SiNWs as nanoantennas to capture, confine, and enhance an optical signal, particularly in the visible range. Significantly, the control of shape and of surface morphology may permit rational design of functional nanostructured material systems with selected spectral and spatial electromagnetic scattering signatures, thereby expanding opportunities for the design of Si-based nano-optical devices and ultracompact optoelectronic circuits.

Acknowledgment. This work was supported in part by the Army Research Office under a Young Investigator Award (W911NF-04-100308) and in part by the NSF Nano-Bio Interface Center at the University of Pennsylvania and Drexel University (DMR-0425780). B.G. was supported by TUBITAK, and E.M.G. and S.S.N. were supported by the NSF GK-12 (DGE-0538476) and the NSF-IGERT (DGE-0221664) programs at Drexel University. L.C. acknowledges partial support from Sigma Xi under a Grant-in-Aid of Research.

Supporting Information Available: (1) Model description for the scattering of a plane wave by an infinitely long cylindrical nanowire; (2) model of the electromagnetic interaction between a SiNW and a AuNC; and (3) comparison of calculated and experimentally observed enhancements for TE-polarized, 632.8 and 785 nm excitation. This material is available free of charge via the Internet at http://pubs.acs.org.

References

(1) Kerker, M. *The Scattering of Light and Other Electromagnetic Radiation*; Academic Press: New York, 1969.
(2) Westphalen, M.; Kreibig, U.; Rostalski, J.; Luth, H.; Meissner, D. *Sol. Energy Mater. Sol. Cells* **2000**, *61*, 97.
(3) Muhlschlegel, P.; Eisler, H. J.; Martin, O. J. F.; Hecht, B.; Pohl, D. W. *Science* **2006**, *308*, 1607.
(4) Engheta, N. *Science* **2007**, *317*, 1698.
(5) Crozier, K. B.; Sundaramurthy, A.; Kino, G. S.; Quate, C. F. *J. Appl. Phys.* **2003**, *94*, 4632−4642.
(6) Xu, H.; Kall, M. *Phys. Rev. Lett.* **2002**, *89*, 246802.
(7) Ozbay, E. *Science* **2006**, *311*, 189.
(8) Fang, N.; Lee, H.; Sun, C.; Zhang, X. *Science* **2005**, *308*, 534.
(9) Bozhevolnyi, S. I.; Volkov, V. S.; Devaux, E.; Laluet, J. Y.; Ebbesen, T. W. *Nature* **2006**, *440*, 508.
(10) Zia, R.; Schuller, J. A.; Chandran, A.; Brongersma, M. L. *Mater. Today* **2006**, *9*, 20.
(11) Tao, A. R.; Sinsermsuksakul, P.; Yang, P. *Nat. Nanotechnol.* **2007**, *2*, 435.
(12) Stockman, M. I. *Phys. Rev. Lett.* **2004**, *93*, 137404.
(13) Seal, K.; Sarychev, A. K.; Noh, H.; Genov, D. A.; Yamilov, A.; Shalaev, V. M.; Ying, Z. C.; Cao, H. *Phys. Rev. Lett.* **2005**, *94*, 226101.
(14) Hanewinkel, B.; Knorr, A.; Thomas, P.; Koch, S. W. *Phys. Rev. B* **1997**, *55*, 13715.
(15) Chew, H.; Wang, D. S. *Phys. Rev. Lett.* **1982**, *49*, 490.
(16) Haes, A. J.; Zou, S.; Schatz, G. C.; Van Duyne, R. P. *J. Phys. Chem. B* **2004**, *108*, 6961.
(17) Biteen, J. S.; Pacifici, D.; Lewis, N. S.; Atwater, H. A. *Nano Lett.* **2005**, *5*, 1768.
(18) Lee, J.; Hernandez, P.; Lee, J.; Govorov, A. O.; Kotov, N. A. *Nat. Mater.* **2007**, *6*, 291.
(19) Kneipp, K.; Wang, Y.; Kneipp, H.; Perelman, L. T.; Itzkan, I.; Dasari, R. R.; Feld, M. S. *Phys. Rev. Lett.* **1997**, *78*, 1667−1670.
(20) Mosbacher, M.; Munzer, H. J.; Zimmermann, J.; Solis, J.; Boneberg, J.; Leiderer, P. *Appl. Phys. A* **2000**, *71*, 1.
(21) Bouhelier, A.; Beversluis, M.; Hartschuh, A.; Novotny, L. *Phys. Rev. Lett.* **2003**, *90*, 013903−013901.
(22) Krasavin, A. V.; MacDonald, K. F.; Schwanecke, A. S.; Zheludev, N. I. *Appl. Phys. Lett.* **2006**, *89*, 031118.
(23) Aspnes, D. E. *Optical Properties of Si*; INSPEC, IEE: London, 1999.
(24) Cao, L.; Laim, L.; Ni, C.; Nabet, B.; Spanier, J. E. *J. Am. Chem. Soc* **2005**, *127*, 13782.
(25) Mohri, N.; Matsushita, S.; Inoue, M.; Yokshikawa, K. *Langmuir* **1998**, *14*, 2343.
(26) Cao, L.; Nabet, B.; Spanier, J. E. *Phys. Rev. Lett.* **2006**, *96*, 157402.
(27) Ditlbacher, H.; Hohenau, A.; Wagner, D.; Kreibig, U.; Rogers, M.; Hofer, F.; Aussenegg, F. R.; Krenn, J. R. *Phys. Rev. Lett.* **2005**, *95*, 257403.
(28) Borselli, M.; Srinivasan, K.; Barclay, P. E.; Painter, O. *Appl. Phys. Lett.* **2004**, *85*, 3693.
(29) Lock, J. A. *J. Opt. Soc. Am., A* **1997**, *14*, 653.
(30) Genov, D. A.; Sarychev, A. K.; Shalaev, V. M. *J. Nonlinear Opt. Phys. Mater.* **2003**, *12*, 1.

NL0729983